Neuroscience 314 (2016) 47–63

ROSUVASTATIN ENHANCES ANTI-INFLAMMATORY AND INHIBITS PRO-INFLAMMATORY FUNCTIONS IN CULTURED MICROGLIAL CELLS

D. KATA,[a] I. FÖLDESI,[b] L. Z. FEHER,[c] L. HACKLER, Jr.[c] L. G. PUSKAS[c] AND K. GULYA[a]*

[a] *Department of Cell Biology and Molecular Medicine, University of Szeged, Szeged, Hungary*

[b] *Department of Laboratory Medicine, University of Szeged, Szeged, Hungary*

[c] *Avidin Ltd., Szeged, Hungary*

Abstract—Microglial activation results in profound morphological, functional and gene expression changes that affect the pro- and anti-inflammatory mechanisms of these cells. Although statins have beneficial effects on inflammation, they have not been thoroughly investigated for their ability to affect microglial functions. Therefore the effects of rosuvastatin, one of the most commonly prescribed drugs in cardiovascular therapy, either alone or in combination with bacterial lipopolysaccharide (LPS), were profiled in pure microglial cultures derived from the forebrains of 18-day-old rat embryos. To reveal the effects of rosuvastatin on a number of pro- and anti-inflammatory mechanisms, we performed morphometric, functional and gene expression studies relating to cell adhesion and proliferation, phagocytosis, pro- and anti-inflammatory cytokine (IL-1β, tumor necrosis factor α (TNF-α) and IL-10, respectively) production, and the expression of various inflammation-related genes, including those related to the above morphological parameters and cellular functions. We found that microglia could be an important therapeutic target of rosuvastatin. In unchallenged (control) microglia, rosuvastatin inhibited proliferation and cell adhesion, but promoted microspike formation and elevated the expression of certain anti-inflammatory genes (*Cxcl1*, *Ccl5*, *Mbl2*), while phagocytosis or pro- and anti-inflammatory cytokine production were unaffected. Moreover, rosuvastatin markedly inhibited microglial activation in LPS-challenged cells by affecting both their morphology and functions as it inhibited LPS-elicited phagocytosis and inhibited pro-inflammatory cytokine (IL-1β, TNF-α) production, concomitantly increasing the level of IL-10, an anti-inflammatory cytokine. Finally, rosuvastatin beneficially and differentially affected the expression of a number of inflammation-related genes in LPS-challenged cells by inhibiting numerous pro-inflammatory and stimulating several anti-inflammatory genes. Since the microglia could elicit pro-inflammatory responses leading to neurodegeneration, it is important to attenuate such mechanisms and promote anti-inflammatory properties, and develop prophylactic therapies. By beneficially regulating both pro- and anti-inflammatory microglial functions, rosuvastatin may be considered as a prophylactic agent in the prevention of inflammation-related neurological disorders.

Key words: anti-inflammation, gene expression, lipopolysaccharide, phagocytosis, pro-inflammation, rosuvastatin.

INTRODUCTION

Microglia, the main immune cells in the central nervous system (CNS), are derived from the monocyte/macrophage lineage (Ginhoux et al., 2010). They play important roles in both physiological and pathophysiological conditions such as traumatic injury, stroke, ischemia or neurodegenerative diseases (Kreutzberg, 1996). In response to activation, the microglia transform from a resting state to an activated form, during which profound morphological and functional changes take place, such as process retraction, proliferation, phagocytosis and cytokine expression (Gehrmann et al., 1995; Kreutzberg, 1996; Hanisch, 2002; Luo and Chen, 2012). Although such anti-inflammatory mechanisms are essential in protecting the CNS, activated microglial cells can also be harmful to neurons by eliciting neuroinflammation that could lead to neurodegeneration (Banati et al., 1993; Gehrmann et al., 1995; Gonzalez-Scarano and Baltuch, 1999; Streit, 2002; Graeber, 2010; Gresa-Arribas et al., 2012; Ghosh et al., 2013). In Alzheimer's disease (AD), for example, the microglia produce pro-inflammatory factors such as interleukin-1β (IL-1β) around the amyloid plaques, and these factors may themselves become important components of the AD pathology because of their ability to increase the expression of amyloid precursor protein (Cordle and Landreth, 2005; Ghosh et al., 2013).

Accumulating evidence indicates that a sequence of events contributes to the development and progression of AD, including oxidative stress, inflammation, and altered cholesterol metabolism (Gamba et al., 2015). Oxidative stress may be crucial in the development of

*Corresponding author. Address: Department of Cell Biology and Molecular Medicine, University of Szeged, 4 Somogyi u., Szeged H-6720, Hungary. Tel: +36-(62)-544-570; fax: +36-(62)-544-569.
E-mail address: gulyak@bio.u-szeged.hu (K. Gulya).

Abbreviations: AD, Alzheimer's disease; Cd, cluster of differentiation; CNS, central nervous system; DIV, days *in vitro*; DMEM, Dulbecco's Modified Eagle's Medium; E18, embryonic day 18; EAE, experimental autoimmune encephalomyelitis; ELISA, enzyme-linked immunosorbent assay; FBS, fetal bovine serum; GAPDH, glyceraldehyde 3-phosphate dehydrogenase (EC 1.2.1.12); Iba1, ionized calcium-binding adaptor molecule 1; IL, interleukin; LPS, bacterial lipopolysaccharide; MS, multiple sclerosis; PBS, phosphate-buffered saline; RT, room temperature; S.D., standard deviation; subDIV, subcloned days *in vitro*; TBS, Tris-buffered saline; TI, transformation index; TNF-α, tumor necrosis factor α.

http://dx.doi.org/10.1016/j.neuroscience.2015.11.053

neuroinflammation as oxidized cholesterol could act as a link connecting peripheral hypercholesterolemia to altered cholesterol metabolism in the brain (Gamba et al., 2015). Cholesterol modulates the processing of amyloid precursor protein and the production of β-amyloid peptides (Shobab et al., 2005), while removing cholesterol ameliorates the production these peptides in animal models (Bodovitz and Klein, 1996; Simons et al., 1998).

Statins (3-hydroxy-3-methylglutaryl coenzyme A reductase inhibitors) are the agents of first choice for the treatment of high cholesterol levels (Taylor et al., 2013). Although their main effects are related to the lipid metabolism (inhibition of cholesterol synthesis, reduction of the levels of low-density lipoproteins and triglycerides, and stimulation of the expression of high-density lipoproteins), they also strongly modulate inflammatory cells around atherosclerotic plaques (Wierzbicki et al., 2003; Burg and Espenshade, 2011). Apart from their therapeutic use in cardiovascular diseases, statins may also have beneficial effects in the CNS (Zipp et al., 2007; van der Most et al., 2009; Famer et al., 2010) as animal studies have demonstrated that statins attenuate neuroinflammation (Zelcer et al., 2007) and reduce senile plaques and inflammatory responses (Kurata et al., 2012).

Interestingly, in spite of being an obvious target for statins, microglial cells have not been at the focus of statin research. There have only been a few studies to demonstrate that under *in vitro* circumstances the microglia respond to statins such as atorvastatin and simvastatin (Lindberg et al., 2005; Nakamichi et al., 2006). In the present study, we investigated the effects of rosuvastatin, the most widely used and arguably the most effective statin (Nissen et al., 2006; Nicholls et al., 2011), on cultured pure microglia cells derived from mixed cultures of 18-day-old embryonic (E18) rat forebrains under control (unstimulated) and bacterial lipopolysaccharide (LPS)-stimulated conditions (Nakamura et al., 1999; Lund et al., 2006; Gresa-Arribas et al., 2012). To reveal the effects of rosuvastatin on a number of pro- and anti-inflammatory mechanisms, we performed morphometric, functional and gene expression studies relating to cell adhesion and proliferation, phagocytic capability, pro- and anti-inflammatory cytokine (IL-1β, tumor necrosis factor α (TNF-α) and IL-10, respectively) production, and the expression of various inflammation-related genes, including those related to the above morphological parameters and cellular functions.

EXPERIMENTAL PROCEDURES

Animals

All animal experiments were carried out in strict compliance with the European Council Directive (86/609/EEC) and EC regulations (O.J. of EC No. L 358/1, 18/12/1986) regarding the care and use of laboratory animals for experimental procedures, and followed the relevant Hungarian and local legislation requirements. The experimental protocols were approved by the Institutional Animal Welfare Committee of the University of Szeged (I-74-II/2009/MÁB). The pregnant Sprague–Dawley rats (45 rats, 170–190 g) were kept under standard housing conditions and fed *ad libitum*.

Antibodies

For a thorough characterization of different microglial phenotypes developed *in vitro*, an antibody against ionized calcium-binding adaptor molecule 1 (Iba1), an intracellular actin- and Ca^{2+}-binding protein expressed in the CNS specifically in macrophages and microglia (Ahmed et al., 2007), was used in our immunocytochemical and Western blot analyses. The anti-glyceraldehyde 3-phosphate dehydrogenase (GAPDH) antibody was used as an internal control in Western blot experiments (Wu et al., 2012). Dilutions of primary and secondary antibodies, and also incubation times and blocking conditions for each antibody used were carefully tested for both immunocytochemistry and Western blot analysis. To detect the specificities of the secondary antisera, omission control experiments (staining without the primary antibody) were performed. In such cases, no fluorescent or Western blot signals were detected.

Cell cultures

Pure microglial cells were isolated from mixed primary cortical cell cultures of rat embryos of either sex by the method we described earlier (Szabo and Gulya, 2013). Sibling embryos obtained from the same pregnancy were processed for culturing together; each pregnancy was considered as an independent experiment. Briefly, 10–12 fetal rats (E18) under anesthesia were decapitated and the frontal lobe of the cerebral cortex was removed, minced with scissors, incubated in 9 ml Dulbecco's Modified Eagle's Medium (DMEM; Invitrogen, Carlsbad, USA) containing 1 g/l D-glucose, 110 mg/l Na-pyruvate, 4 mM L-glutamine, 3.7 g/l $NaHCO_3$, 10,000 U/ml penicillin G, 10 mg/ml streptomycin sulfate, 25 μg/ml amphotericin B and 0.25% trypsin for 10 min at 37 °C, and then centrifuged at 1000*g* for 10 min at room temperature (RT). The pellet was resuspended and washed twice in 5 ml DMEM containing 10% heat-inactivated fetal bovine serum (FBS; Invitrogen) and centrifuged for 10 min at 1000*g* at RT. The final pellet was resuspended in 2 ml DMEM/10% FBS, after which the cells were plated in the same medium on a poly-L-lysine-coated culture flask (75 cm^2, 12×10^6 cell/flask) and cultured at 37 °C in a humidified air atmosphere supplemented with 5% CO_2, in one or other of the following ways: (1) in poly-L-lysine-coated coverslips (15 × 15 mm; 2×10^5 cells/coverslip) for immunocytochemistry; (2) in poly-L-lysine-coated Petri dishes (60 mm × 15 mm; 4×10^5 cells/dish) for Western blot analyses and enzyme-linked immunosorbent assay (ELISA) studies; or (3) in a poly-L-lysine-coated culture flask (75 cm^2, 12×10^6 cells/flask) for the subsequent generation of pure microglial cell cultures.

Secondary microglial cells were subcloned from mixed primary cultures (DIV7) maintained in a poly-L-lysine-coated culture flask (75 cm^2, 12×10^6 cells/flask) by shaking the cultures at 100 rpm in a platform shaker for 30 min at 37 °C. Cultures from the same pregnancy were kept separate. Microglia from the supernatant

were collected by centrifugation at 3000*g* for 8 min at RT and resuspended in 2 ml DMEM/10% FBS. The cells were seeded at a density of 4×10^5 cells/Petri dish for Western blots or 2×10^5 cells/coverslip/Petri dish for immunocytochemistry, proliferation or phagocytosis assays, and cultured in DMEM in a humidified atmosphere supplemented with 5% CO_2 at 37 °C. The medium was changed on the first day after seeding (subDIV1). Immunocytochemistry routinely performed on the pure microglial cultures four days after seeding (subDIV4) consistently detected a >99% incidence of the Iba1-immunopositive microglial cells for the Hoechst 33258 dye-labeled cell nuclei.

Cell culture treatments

On the fourth day of subcloning (subDIV4), DMEM was replaced and the expanded pure microglial cells were treated for 24 h with either LPS (20 ng/ml final conc., dissolved in DMEM; Sigma, St. Louis, MO, USA) or rosuvastatin (1 μM final conc., dissolved in sterile, distilled water; Santa Cruz Biotechnology, Inc., Dallas, TX, USA) alone, or with a combination of LPS + rosuvastatin, and the effects were compared in a variety of morphological and functional tests. LPS treatment served as an immunochallenge. Four types of treatment regimens were used: (1) control (unchallenged and untreated) cultures; (2) LPS-challenged cultures received 20 ng/ml LPS; (3) rosuvastatin-treated cultures were stimulated with 1 μM rosuvastatin; (4) LPS-challenged + rosuvastatin-treated cultures received both drugs in the indicated doses. Depending on the experiments, the treatments lasted for 6, 24 or 72 h at 37 °C.

Cell adhesion and proliferation

To measure changes in cell adhesion and proliferation and cell viability, the ACEA Real-Time Cell Analysis (RTCA) system and 16-well E-Plates (Acea Biosciences, Inc., San Diego, CA, USA) were used. This system measured the electrical impedance of the cells expressed as cell index in real time. Briefly, 4×10^5 pure microglial cells in poly-L-lysine-coated Petri dishes were plated as described above. On the fourth day of culturing, the cells were trypsinized, centrifuged as above and seeded into gelatin-coated 16-well E-Plates at a density of 6000 cells per well. Test doses of LPS and rosuvastatin, either alone or in combination, were added to the wells before plating. After equilibration at RT for 10 min, the E-plate was loaded into the RTCA machine and the cell index was measured continuously for 60 h using the cell microelectronic sensing technique with the xCELLigence real-time cell analysis system (RTCA DP; Acea Biosciences) as we published earlier (Ozsvári et al., 2010). Cell indices at 24 h were analyzed for comparison with cell proliferation data. Data analysis was carried out with the system's dedicated software (RTCA Software 1.2; Acea Biosciences) and Excel (Microsoft Corp., Redmond, WA, USA). To estimate the number of surviving/proliferating microglial cells after treatments, the cultures were washed twice with 2 ml phosphate-buffered saline (PBS) to remove cell debris, treated with 0.25% trypsin solution for 10 min at 37 °C, collected and counted in a Burker cell counting chamber. The number of viable cells was presented as mean ± S.D.

Immunocytochemistry

Pure microglial cultures treated with different treatment regimens were fixed on coverslips with 4% formaldehyde for 5 min and rinsed with 0.05 M PBS for 2×5 min. After permeabilization and blocking of the nonspecific sites in 0.05 M PBS solution containing 5% normal goat serum (Sigma), 1% heat-inactivated bovine serum albumin (Sigma) and 0.05% Triton X-100 for 30 min at 37 °C, the cells on the coverslips were incubated overnight in a humidified chamber at 4 °C with rabbit anti-Iba1 polyclonal antibody (1:500 final dilution; Wako, Japan), a microglia-specific actin-binding protein, in the above solution as we described previously (Szabo and Gulya, 2013). The cultured cells were washed for 4×10 min at RT in 0.05 M PBS, and then incubated with the Alexa Fluor 568 fluorochrome-conjugated goat anti-rabbit antibody (1:1000 final dilution; Invitrogen) in the dark for 3 h at RT. The cells on the coverslip were washed for 4×10 min in 0.05 M PBS at RT, and the nuclei were stained in 0.05 M PBS solution containing 1 mg/ml polyvinylpyrrolidone and 0.5 μl/ml Hoechst 33258 dye (Sigma). The coverslips were rinsed in distilled water for 5 min, air-dried and mounted on microscope slides in Vectashield mounting medium (Vector Laboratories, Burlingame, CA, USA). Cells were viewed on a Nikon Microphot-FXA epifluorescent microscope (Nikon Corp., Tokyo, Japan) and photographed with a Spot RT Color CCD camera (SPOT RT/ke, Diagnostic Instruments, Inc., Sterling Heights, MI, USA).

Western blot analysis

Cultured microglial cells (subDIV4) were collected through use of a rubber policeman, homogenized in 50 mM Tris–HCl (pH 7.5) containing 150 mM NaCl, 0.1% Nonidet P40, 0.1% cholic acid, 2 μg/ml leupeptin, 1 μg/ml pepstatin, 2 mM phenylmethylsulfonyl fluoride and 2 mM EDTA, and centrifuged at 10,000*g* for 10 min. The pellet was discarded and the protein concentration of the supernatant was determined (Lowry et al., 1951). For the Western blot analyses, 5–10 μg of protein was separated on an SDS polyacrylamide gel (4–10% stacking gel/resolving gel), transferred onto Hybond-ECL nitrocellulose membrane (Amersham Biosciences, Little Chalfont, Buckinghamshire, England), blocked for 1 h in 5% nonfat dry milk in Tris-buffered saline (TBS) containing 0.1% Tween 20, and incubated overnight with either a rabbit anti-Iba1 polyclonal antibody (1:1000 final dilution; Wako) or a mouse anti-GAPDH monoclonal antibody (clone GAPDH-71.1; 1:20,000 final dilution; Sigma). After five rinses in 0.1% TBS–Tween 20, the membranes were incubated for 1 h with the peroxidase-conjugated goat anti-rabbit secondary antibody (1:2000 final dilution; Invitrogen) for Iba1 or with the peroxidase-conjugated rabbit anti-mouse secondary antibody (1:2000 final dilution;

Sigma) for GAPDH Western blots, and washed five times as before. The enhanced chemiluminescence method (ECL Plus Western blotting detection reagents; Amersham Biosciences) was used to reveal immunoreactive bands according to the manufacturer's protocol.

In vitro phagocytosis

The fluid-phase phagocytotic capabilities of the control and variously treated pure microglial cell cultures were determined via the uptake of fluorescent microspheres (carboxylate-modified polystyrene beads, fluorescent yellow-green (λex ~470 nm; λem ~505 nm), aqueous suspension, 2.0 μm mean particle size; L4530, Sigma) as we described previously (Szabo and Gulya, 2013). Unstimulated (control) and LPS-stimulated pure microglial cell cultures (subDIV4) with or without rosuvastatin were tested for 24 h. At the end of the treatment period, 1 μl of a 2.5% aqueous suspension of fluorescent microspheres per ml was added to the culture, which was then incubated for 60 min at 37 °C. The cells were next washed five times with 2 ml of PBS to remove dish- or cell surface-bound residual fluorescent microspheres, and fixed with 4% formaldehyde in PBS. In another setup, we also determined the number of microglial cell membrane-associated but not phagocytosed beads. Such negative controls were treated as above with the exception that microglial cultures with beads were incubated for 60 min at 4 °C. At this temperature, the number of beads associated with cell surface averaged less than 1 bead per 100 Iba1-labeled cells, thus the phagocytosis was not considered significant. For measurement of the phagocytotic activity, cells labeled with phagocytosed microbeads and processed for Iba1 immunocytochemistry were counted in 20 random fields in each treatment group (mean ± S.D.) under a 20× or 40× objective. Statistically significant differences were determined by a two-way ANOVA.

Determination of IL-1β, IL-10 and TNF-α

For ELISA assays, the supernatants were collected from each treatment and stored at −20 °C. Concentrations of IL-1β, IL-10 and TNF-α were measured with rat-specific ELISA kits (eBioscience, Vienna, Austria). The sensitivity of IL-1β (Cat# BMS630), IL-10 (Cat# BMS629) and TNF-α (Cat#BMS622) assays was 4 pg/ml, 1.5 pg/ml and 11 pg/ml, respectively. As stated by the manufacturer, the overall intra- and interassay coefficients of variation were < 10% in both cases for IL-1β and TNF-α, and < 5% in both cases for IL-10.

RNA isolation

Total RNA from control and treated pure microglial cells was purified as described previously (Fabian et al., 2011); columns and wash buffer were from Bioneer (Viral RNA extraction kit; Daejon, South Korea). Briefly, cells were washed with PBS, incubated in lysis buffer (RA1; Macherey-Nagel, Düren, Germany), then collected and mixed with 70% ethanol in RNase-free water (Bioneer). The mixture was transferred through columns (Bioneer) and washed with 350 μl 80% ethanol in diethyl pyrocarbonate-treated water, and then with 600 μl and 300 μl W2 wash buffer (Bioneer). Total RNA was eluted in 50 μl RNase free-water. One μl RNase inhibitor (Applied Biosystems, Foster City, CA, USA) was added to the samples. The quality and quantity of the isolated RNA were measured with NanoDrop1000 Version 3.8.1. (Thermo Scientific, Budapest, Hungary).

RNA expression

Reverse transcription from 3 μg of total RNA in 30 μl was performed with the High-Capacity cDNA Archive Kit (Applied Biosystems) according to the manufacturer's protocol. cDNA was diluted to 80 μl. The instrumentation included the Bravo automatic liquid handling system (Agilent Technologies, Inc., Santa Clara, CA, USA) for polymerase chain reaction (PCR) assay preparation and a LightCycler 1536 System (Roche Diagnostics Corp., Indianapolis, IN, USA) or a Light Cycler Nano Instrument (Roche) for cycling (Woudstra et al., 2013). The expression of 116 inflammation-related genes, together with that of six control genes (see below), was measured with Universal Probe Library assays using intron-spanning gene-specific primers (Rat Immune Panel; Avidin Ltd., Szeged, Hungary, www.avidin-biotech.com/services/gene-expression) and the LightCycler 1536 DNA Probe Master kit (Roche). Moreover, the expression of certain phagocytosis-related genes such as the integrin-associated protein or cluster of differentiation 47 (*Cd47*, NM_019195_2), the engulfment or cell motility protein (*Elmo1*, NM_001108415.1), the scavenger receptor class B member 1 (*Scarb1*, NM_031541_1), the plasminogen activator inhibitor-1 (*Serpine1*, NM_012620_1), the signal-regulatory protein α (*Sirpa,* NM_013016_2) and the vesicle-associated membrane protein 7 (*Vamp7*, NM_053531_1) were also analyzed, by the Light Cycler Nano Instrument. For the 1536 System, each 2 μl PCR reaction contained 8 ng of cDNA, 0.4 μl Lightcycler DNA Probes Master (5×), the corresponding primer set and UPL probe and the Setup Control. The PCR cycling protocol was as follows: enzyme activation at 95 °C for 60 s, 50 cycles of denaturation at 95 °C for 0 s, and annealing and extension at 60 °C for 30 s. For the Nano Instrument, each 20 μl PCR reaction contained 20 ng cDNA, 10 μl Lightcycler DNA Probes Master (5×), the corresponding primer set and UPL probe and the Setup Control. The PCR protocol was as follows: enzyme activation at 95 °C for 10 min, 50 cycles of denaturation at 95 °C for 15 s, and annealing and extension at 60 °C for 30 s. Gene expression was normalized to the average values of clathrin, heavy chain (*Cltc*, NM_019299.1), glyceraldehyde-3-phosphate-dehydrogenase (*Gapdh*, M17701.1), glucuronidase, beta (*Gusb*, NM_017015.2), hypoxanthine phosphoribosyltransferase 1 (*Hprt1*, NM_012583.2), phosphoglycerate kinase 1 (*Pgk1*, NM_053291.3), and tubulin, beta 5 class I (*Tubb5*, NM_173102.2) expression as endogenous controls and expressed relative to the unstimulated controls by using the $2^{-\Delta\Delta Ct}$ method. A total of 122 gene-specific assays were run on four independent samples from each condition. Student's *t*-test and a two-way ANOVA were applied for the analysis of significance where $p < 0.05$ was

considered significant. For hierarchical cluster analysis and visualization, the Hierarchical Clustering Explorer (v3.0) software was used (publicly available at http://www.cs.umd.edu/hcil/multi-cluster/hce3.html). The complete linkage clustering method was applied with Euclidean distance metric.

Image analysis and statistics

Digital images were captured by a Nikon Microphot-FXA epifluorescent microscope (Nikon Corp., Tokyo, Japan), using a Spot RT Color CCD camera and the Spot RT software (Spot RT/ke Diagnostic Instruments, Sterling Heights, MI, USA). For the determination of microglial cell purity, Hoechst 33258-labeled cell nuclei that belonged to Iba1-immunopositive cells were counted on coverslip-cultured samples. For each culture, 50–100 randomly selected microscope fields were analyzed. In every case, the cultures had, on average, at least 99 Iba1-positive somata for 100 Hoechst 33258-labeled cell nuclei (>99% purity for microglial cells). Phagocytosed microspheres on 20 randomly sampled microscope fields from three coverslips for each treatment regimen were counted with the use of the computer program ImageJ (version 1.47; http://rsb.info.nih.gov/ij). For the measurement of area (μm^2), perimeter (μm) and transformation index (TI), Iba1-immunoreactive microglial cell images were converted into binary replicas by using thresholding procedures implemented by ImageJ and Adobe Photoshop CS5.1 software (Adobe Systems, Inc., San Jose, CA, USA) as published by Szabo and Gulya (2013). TI was determined according to Fujita et al. (1996) by using the following formula: [perimeter of cell $(\mu m)]^2/4\pi$ [cell area (μm^2)]. Color correction and cropping of the light microscopic images were performed when photomicrographs were made for publication and assembled for a panel. Gray-scale digital images of the immunoblots were acquired by scanning the autoradiographic films with a desktop scanner (Epson Perfection V750 PRO; Seiko Epson Corp., Japan). The images were scanned and processed at identical settings to allow comparisons of the Western blots from different samples. The bands were analyzed through the use of ImageJ. The immunoreactive densities of equally loaded lanes were quantified, and all samples were normalized to the internal GAPDH load controls.

All statistical comparisons were made by using R 3.1.0 for Windows (The R Foundation for Statistical Computing; Wirtschafts-Universität, Wien, Austria). Results were analyzed with a two-way ANOVA, and the Bonferroni correction was used to establish significance between groups. Values were presented as mean ± S.D.; $p < 0.05$ was considered significant; *, ** and *** denote $p < 0.05$, $p < 0.01$ and $p < 0.001$, respectively.

RESULTS

Rosuvastatin affects microglial morphology

The morphological changes elicited by rosuvastatin in unchallenged (control) and LPS-challenged pure microglia cultures were documented through the use of Iba1 immunocytochemistry (Fig. 1A–D) and quantitatively analyzed on binary silhouettes of individual microglial cells (Fig. 2A–G). Iba1 protein expression was also monitored during treatments (Fig. 1E). Most of the unchallenged and untreated (control) microglia displayed ameboid morphology with TI < 3; they had a predominantly ameboid shape, occasionally with small pseudopodia (Figs. 1A and 2A). When administered alone for 24 h, rosuvastatin induced the formation of numerous microspikes (Figs. 1B and 2*B*); these slender cytoplasmic projections (filopodia) resulted in significantly increased perimeter and TI values of these cells (Fig. 2F, G). Quantitative analysis showed that the average TI in this group increased about 10-fold, to above 19, as compared with the controls (Fig. 2G). The LPS challenge did not result in any significant morphometric change (Figs. 1C and 2C, E–G). However, rosuvastatin treatment in LPS-challenged cells resulted in a significantly enlarged and more ramified cell form (TI > 7) with a much larger perimeter value as compared with their respective control values (Figs. 1D and 2D, E–G), indicating that rosuvastatin profoundly antagonized the morphological changes characteristic of LPS-induced microglial activation. In relation to the substantially increased size of the LPS-challenged and rosuvastatin-treated microglia (Figs. 1D and 2D, E), their Iba1 immunoreactivity was also significantly increased (Figs. 1E and 2E).

Rosuvastatin inhibits proliferation and cell adhesion in both unchallenged and LPS-challenged microglia

Rosuvastatin significantly inhibited cell proliferation in both unchallenged and LPS-challenged cultures, by 47.8% and 68.9%, respectively, after a 24-h treatment period (Fig. 3A). We used a 16-well E-Plate-based real-time analysis to determine whether rosuvastatin affects cell adhesion. Rosuvastatin inhibited cell adhesion in both unchallenged (control) and LPS-challenged microglia (Fig. 3B). The differences in levels of inhibition of cell adhesion between cultures with or without rosuvastatin (unchallenged and LPS-challenged microglia vs. rosuvastatin-treated and LPS-challenged + rosuvastatin-treated microglia) were significant by 20 h of culturing and thereafter, probably due to the significantly larger cell populations in the control and LSP-challenged microglial cultures as compared with those in the rosuvastatin or LPS + rosuvastatin-treated cultures (Fig. 3B), and to the ability of rosuvastatin to stimulate the formation of microspikes (Fig. 2B, D), i.e. the actin-based filamentous protrusions implicated in the cell motility, and consequently in the decreased adhesion of these cells.

Rosuvastatin reduces phagocytotic activity in LPS-challenged cells

The microglial function is inherently related to its phagocytotic activity. In pure microglial cultures (subDIV4), the control (unchallenged and untreated) microglia exhibited a low level of fluid-phase

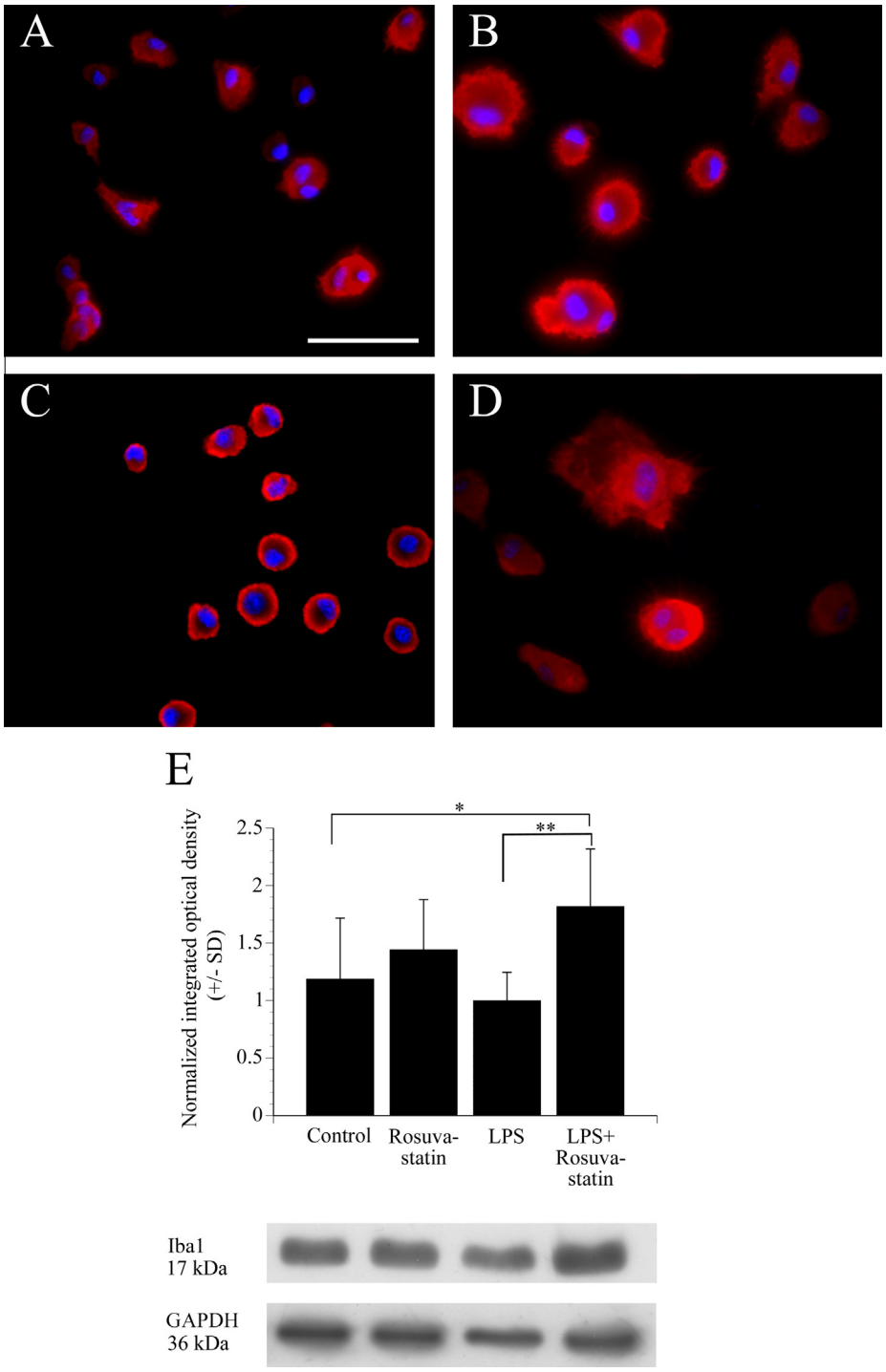

Fig. 1. Rosuvastatin affects microglial cell morphology and Iba1 immunoreactivity in pure microglial cells after various treatments. Pure microglia cell cultures (subDIV4) were maintained as described in Experimental procedures. (A–D) Representative fluorescent immunocytochemical pictures demonstrate the typical cellular distribution of Iba1 immunoreactivity (red) in (A) control (unchallenged and untreated), (B) rosuvastatin-treated, (C) LPS-challenged and (D) LSP-challenged + rosuvastatin-treated microglial cells. The effects of rosuvastatin in unchallenged and LSP-challenged microglia were the most marked. Hoechst 33258-labeled cell nuclei are shown in blue. Scale bar in A (for all pictures): 50 μm. (E) Quantitative Western blot analysis of Iba1 and GAPDH immunoreactivities in pure microglial cell cultures. Protein samples from the cultures were separated by gel electrophoresis, transferred to nitrocellulose membranes and probed with either the Iba1 or the GAPDH antibody. Gray-scale digital images of the immunoblots were acquired by scanning the autoradiographic films with a desktop scanner. The images were scanned and processed at identical settings to allow comparisons between the Western blots from different samples. Error bars indicate integrated optical density values (mean ± SD) normalized to the internal standard GAPDH. Representative Western blot pictures are shown below the graphs. Data were analyzed with a two-way analysis of variance (ANOVA). $^{*}p < 0.05$, $^{**}p < 0.01$. (For interpretation of the references to colour in this figure legend, the reader is referred to the web version of this article.)

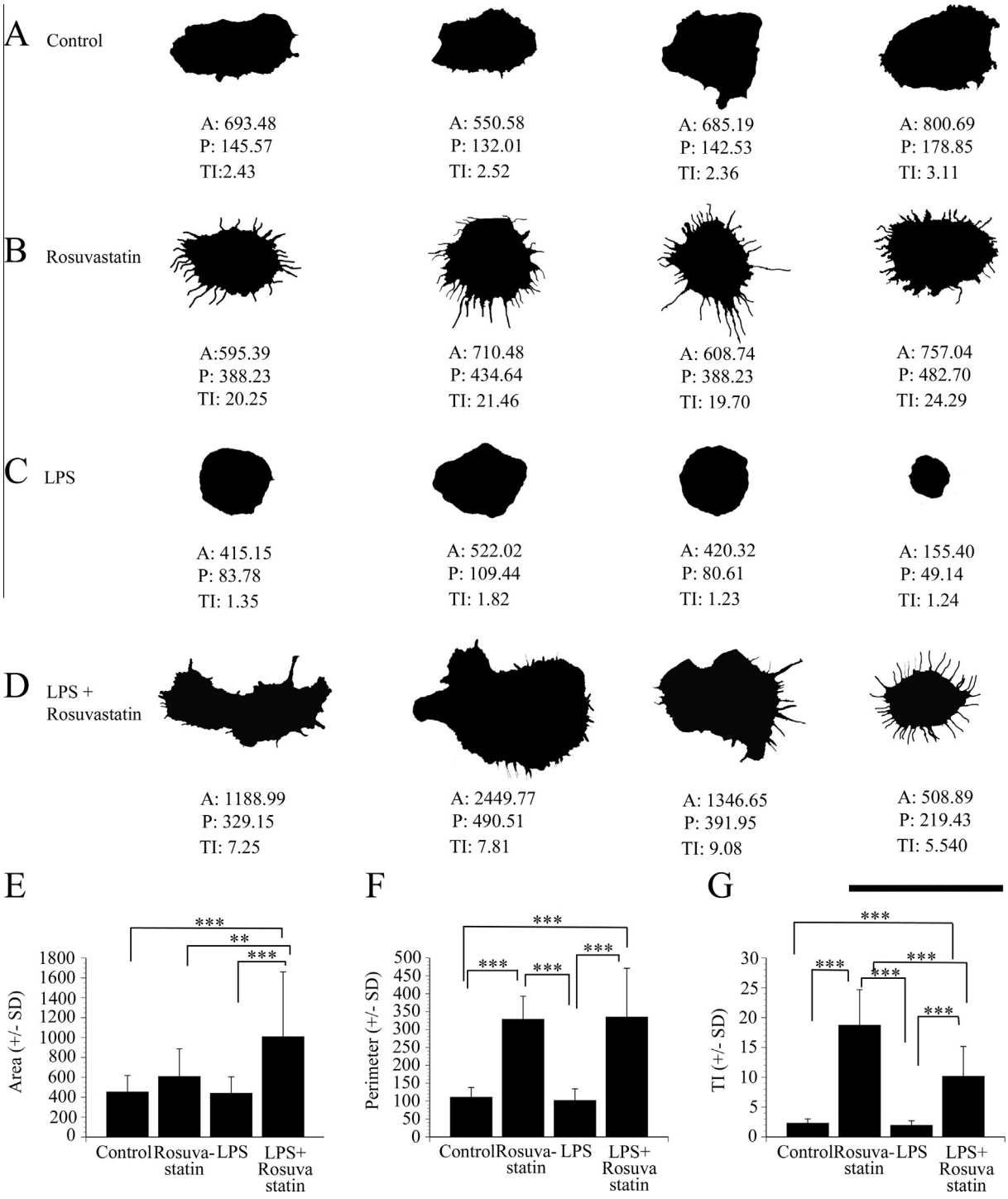

Fig. 2. Quantitative analysis of microglial morphology in pure microglial cell cultures after various treatments. Pure microglial cell cultures (subDIV4) were maintained as described in the Experimental procedure. (A–D) Iba1-positive microglial cells from pure microglial cultures (subDIV4) were photographed, the pictures were digitized and the morphological characteristics were quantitatively analyzed on binary silhouettes of unchallenged (A), rosuvastatin-treated (B), LPS-challenged (C) and LCS-challenged + rosuvastatin-treated (D) microglia. Four representative binary silhouettes are shown for each culturing protocol. Scale bar for all silhouettes: 50 μm. Area (E) in μm^2, perimeter (F) in μm, and TI values (G), calculated as [perimeter of cell (μm)]^2/4π[cell area (μm^2)], are indicated for each digitized cell. Unchallenged and untreated (control) cells, similarly to LPS-challenged cells, displayed a typical ameboid morphology with low TI values. Rosuvastatin affected the morphology of both the control and the LPS-challenged microglia (B, D). In unchallenged cultures, it promoted microspike formation with a concurrent slight ramification of the cells (B). In the LPS-challenged + rosuvastatin-treated cultures (D), the microglia became larger and, while retaining microspikes, also developed thicker processes. Both the rosuvastatin treatment alone and the combined treatment with LPS resulted in larger perimeter (F) and higher TI values (G) as compared with both the unchallenged and the LPS-challenged cultures. (E) Average area (in μm^2 ± S.D.) measurements for cultured pure microglial cells. (F) Average perimeter (in μm ± S.D.) measurements for cultured pure microglial cells. (G) Average TI values (± S.D.) for cultured pure microglial cells. LPS: 20 ng/ml; rosuvastatin: 1 μM. For (E–G), error bars indicate mean ± SD of six replicate measurements from three independent culturings. Data were analyzed with a two-way analysis of variance (ANOVA). $^{**}p < 0.01$; $^{***}p < 0.001$.

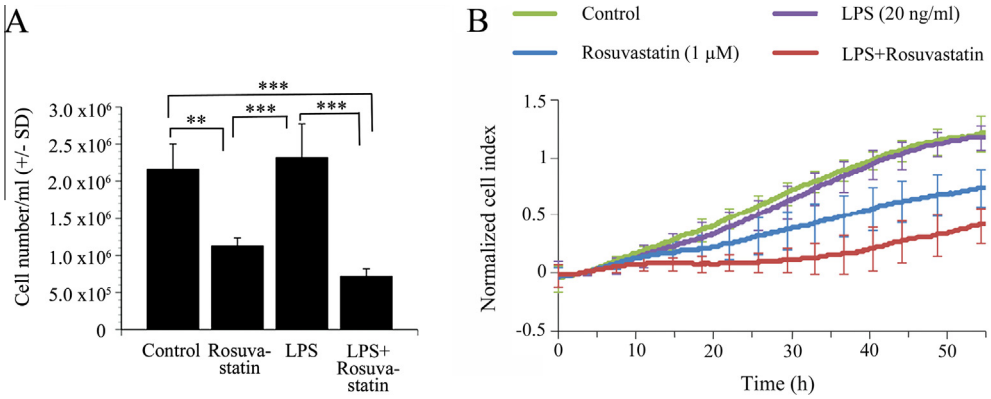

Fig. 3. Rosuvastatin inhibits cell proliferation and decreases cell adhesion. Pure microglial cultures (subDIV4) were maintained and treated as described in Experimental procedures section. (A) After culturing, the cells were collected and the number of surviving microglia was determined with a Bürker chamber. Rosuvastatin, in both unchallenged and LPS-challenged cultures, inhibited cell proliferation and displayed a strong anti-mitotic characteristic. LPS treatment did not affect cell proliferation. (B) Real-time monitoring of microglial cell adhesion after different treatment regimens. The ACEA Real-Time Cell Analysis (RTCA) system and 16-well E-Plates were used to determine cell indices as described in Experimental procedures section. Normalized cell index values are plotted as a function of time. In both unchallenged and LPS-challenged cells, rosuvastatin decreased cell adhesion (blue and red lines, respectively). Error bars indicate mean ± SD of six replicate measurements from three independent culturings. Data were analyzed with a two-way analysis of variance (ANOVA). $^{**}p < 0.01$; $^{***}p = 0.001$. (For interpretation of the references to colour in this figure legend, the reader is referred to the web version of this article.)

phagocytosis (Fig. 4A, E), engulfing only 2.62 ± 1.7 beads per cell ($n = 91$). Rosuvastatin did not affect the phagocytosis appreciably (Fig. 4B, E), the number of phagocytosed microbeads remaining low (2.70 ± 1.7; $n = 50$). As expected, the LPS challenge increased the phagocytotic activity of the microglial cells significantly (Fig. 4C, E). On average, the LPS-challenged cells accumulated 25.39 ± 11.4 beads per cell ($n = 70$), and some of the cells engulfed as many as 40 microbeads. In the LPS-challenged microglia, however, rosuvastatin inhibited the phagocytosis drastically, by nearly 80% (Fig. 4D, E) as the fluid-phase phagocytotic activity was returned close to the level of the control cells (4.67 ± 3.9 microbeads per cell; $n = 88$). As activated microglial cells often damage neuronal tissue, such a strong inhibition of a pro-inflammatory action by rosuvastatin could be beneficial in preventing or ameliorating neurodegeneration.

Rosuvastatin concomitantly decreases pro-inflammatory and increases anti-inflammatory cytokine levels

Activated microglia are known to express several pro- and anti-inflammatory cytokines, while statins are able to reduce the inflammatory effect in the vicinity of atherosclerotic plaques. We therefore expected rosuvastatin to regulate the amount of cytokines released by the microglia. Indeed, when the basal levels of the pro-inflammatory cytokines IL-1β and TNF-α and the anti-inflammatory cytokine IL-10 in unchallenged microglia were compared with the levels from rosuvastatin-treated LPS-challenged or unchallenged cells, a unique regulatory pattern emerged (Fig. 5). The basal level for IL-1β in unchallenged (control) microglia was 15.00 ± 5.6 pg/ml (Fig. 5A). Rosuvastatin did not change this level significantly (9.56 ± 13.1 pg/ml). As expected, a 24 h-long LPS challenge significantly elevated the IL-1β level in the activated microglia, to 156.05 ± 63.0 pg/ml. However, when added together with LPS, rosuvastatin significantly inhibited the development of this elevated IL-1β level, by about 45%, to 86.25 ± 49.3 pg/ml. A similarly strong effect of rosuvastatin was demonstrated on the level of TNF-α, another pro-inflammatory cytokine, in LPS-challenged microglial cells (Fig. 5B). Two different treatment times (6 h and 24 h) were used as the TNF-α production responded quickly to the LPS challenge. The level of TNF-α in the unchallenged (control), rosuvastatin-treated microglia could not be detected, but its level quickly rose, to 906.80 ± 281.7 pg/ml in the LPS-challenged cells after 6 h, and the level was still robust after 24 h (188.19 ± 38.6 pg/ml). When rosuvastatin was co-administered to LPS-challenged cells for either 6 h or 24 h, it significantly inhibited the production of TNF-α, by 39% and 40%, respectively (Fig. 5B).

Moreover, rosuvastatin affected the production of IL-10, an anti-inflammatory cytokine (Fig. 5C). The basal and rosuvastatin-treated levels of IL-10 in the unchallenged microglia were not significantly different (37.01 ± 18.4 pg/ml vs. 75.32 ± 35.4 pg/ml), although elevated IL-10 production was noted after rosuvastatin treatment. Interestingly, LPS increased the IL-10 protein expression significantly to about 340% of the level of the unchallenged microglia (125.3 ± 25.3 pg/ml pg/ml). When rosuvastatin was co-administered with LPS, it boosted the IL-10 protein expression even higher, to about 750% of the basal level (276.84 ± 85.6 pg/ml), indicating the very strong anti-inflammatory action of rosuvastatin.

Rosuvastatin affects the expression of inflammation-related genes

When the profound morphological and functional effects of rosuvastatin on the pro- and anti-inflammatory

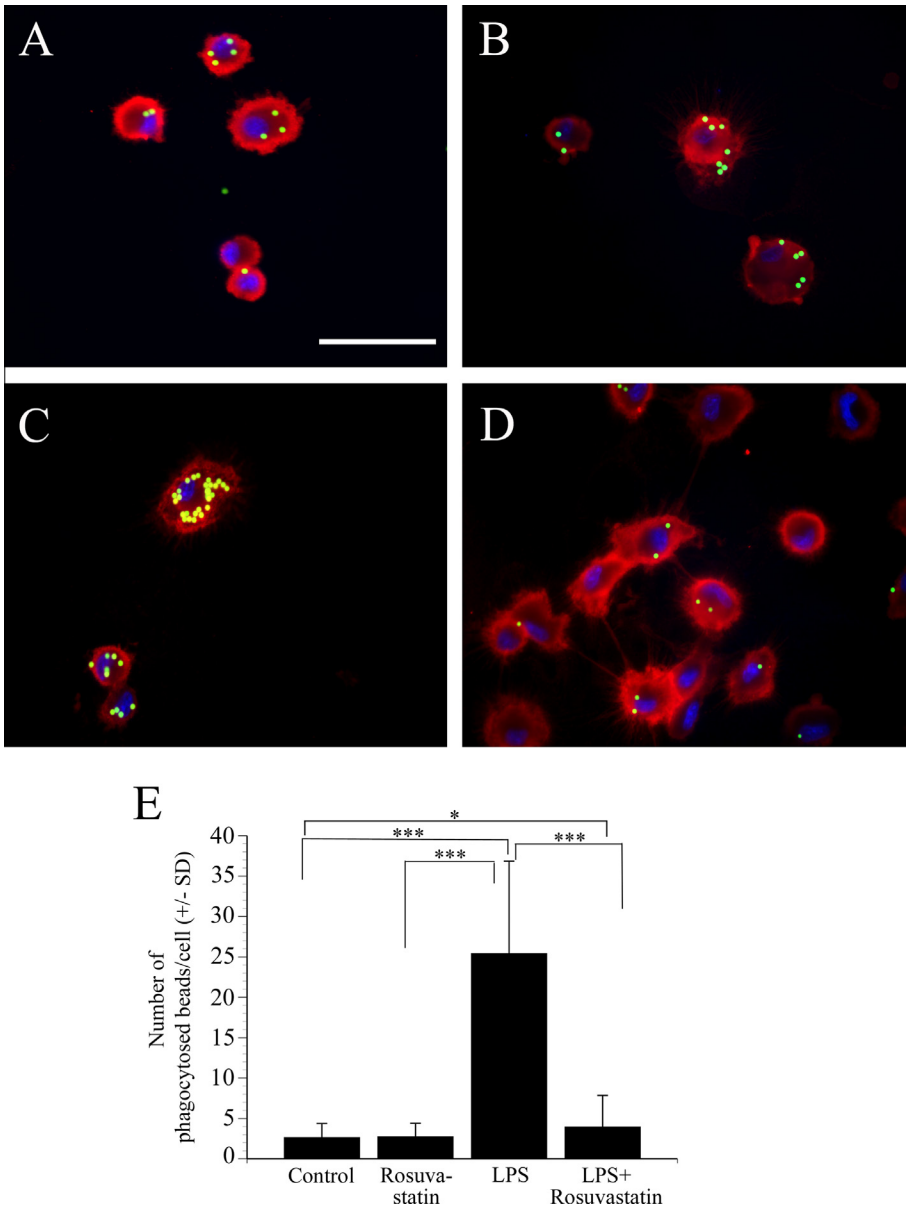

Fig. 4. Rosuvastatin is a potent inhibitor of phagocytosis. Pure microglial cultures (subDIV4) were maintained and treated with fluorescent microbeads (2 μm in diameter) as described in Experimental procedures section. Iba1-specific fluorescent immunocytochemistry (red: microglia; blue: nucleus; green: microspheres) on unchallenged (A), rosuvastatin-treated unchallenged cells (B), LPS-challenged cells (C) and LPS-challenged + rosuvastatin-treated microglial cells (D) revealed that rosuvastatin inhibited phagocytosis in both naive, unchallenged (B) and LPS-challenged cells (D). Scale bar in A (for all pictures) = 50 μm. (E) Quantitative analysis of the number of phagocytosed microbeads revealed that LPS dramatically activated phagocytosis, while rosuvastatin when present significantly decreased this microglial function. Error bars indicate mean ± SD of six replicate measurements from three independent culturings. Data were analyzed with a two-way ANOVA. $^{*}p < 0.05$, $^{***}p < 0.001$. (For interpretation of the references to colour in this figure legend, the reader is referred to the web version of this article.)

capabilities of the microglia had become apparent, we set out to analyze the effects of rosuvastatin on the expression of 122 inflammation-related genes in unchallenged and LPS-challenged pure microglial cells. The hierarchical cluster analysis of 75 such genes is summarized in Fig. 6, and the genes with 47 of the most noteworthy and significant expression changes in response to treatment are listed in Table 1. The results of the analysis indicated that treatment with 1 μM rosuvastatin in unchallenged and LPS-challenged microglia could induce either the upregulation or the downregulation of a number of genes. Levels of expression of selected inflammation-related genes (for example, *Ccl24*, *Ccr1*, *IL-11*, *Cxcl1*, *Ccl4*, *Ccl5*, *Hspb1*, *TGFb-2* and *Mbl2)* are highlighted in Fig. 7. Some of these genes responded to rosuvastatin in unchallenged or challenged cells, or were affected by the LPS challenge. The genes upregulated by the LPS challenge included those coding for chemokine ligands 1, 2, 4, 5, 9, 19 and 24 (*Cxcl1* = 111.6-fold, *Ccl2* = 34.5-fold, *Ccl4* = 17.6-fold, *Ccl5* = 147.0-fold, *Cxcl9* = 118.2-fold, *Ccl19* = 5.2-fold and *Ccl24* = 24.6-fold), IL-11

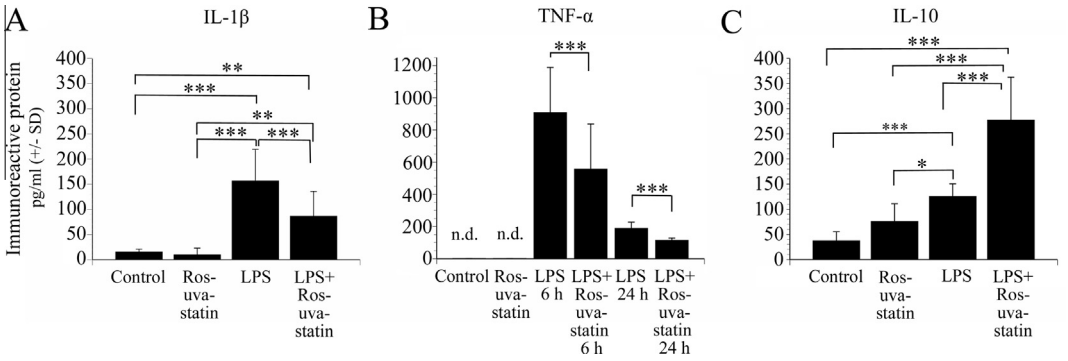

Fig. 5. Rosuvastatin reduces the pro-inflammatory cytokine IL-1β and TNF-α levels and increases the anti-inflammatory IL-10 production. Pure microglial cultures (subDIV4) were maintained and treated as described in Experimental procedures section. After treatments for 6 or 24 h, immunoreactive protein levels (pg/ml ± S.D.) for IL-1β (A), TNF-α (B) and IL-10 (C) were detected by ELISA. TNF-α production was measured after 6 h and 24 h (B). As expected, pro-inflammatory cytokine production was significantly increased in the LPS-challenged cells (A, B). Rosuvastatin was a potent inhibitor of this effect for both IL-1β (A) and TNF-α (B). The level of the anti-inflammatory cytokine IL-10 was measured after 24 h (C). Rosuvastatin slightly increased the level of IL-10 both in unchallenged and in LPS-challenged microglia, to 750% of the control level in the latter case (C). Error bars indicate mean ± S.D. of six replicate measurements from three independent culturings. Data were analyzed with a two-way ANOVA. n.d. = not detected. $^{*}p < 0.05$; $^{**}p < 0.01$; $^{***}p < 0.001$.

(*Il11* = 19.3-fold), IL-23 receptor (*Il23r* = 246.6-fold) and mannose-binding lectin (protein C) two receptor (*Mbl2* = 33.2-fold). Only a few genes were downregulated by the LPS challenge, the most affected one being that of the myosin regulatory light chain 2 (*Myl2* = −4.4-fold).

Rosuvastatin treatment in unchallenged cells affected fewer, but similarly important microglial genes involved in pro- and anti-inflammatory processes. The genes upregulated by rosuvastatin included *Cxcl1* (7.0-fold; Fig. 7D), the anti-inflammatory *Ccl5* (6.6-fold; Fig. 7F), and, most importantly, *Mbl2* (126.2-fold; Fig. 7I), a crucial factor in the development of innate immunity (Worthley et al., 2005). Rosuvastatin was in general a weak inhibitor of the expression of inflammatory genes as it downregulated only a few genes, notably the anti-inflammatory interleukin-10 (*Il10* = −4.0-fold) and the pro-inflammatory chemokine (C–C motif) receptor 1 (*Ccr1* = −2.9-fold). When rosuvastatin was applied to LPS-challenged cultures (Table 1, Figs. 6 and 7), a more complex picture emerged. Some of the LPS-upregulated genes were inhibited by rosuvastatin, as seen in the case of *Ccl24*, where a substantial, 377% decrease in gene expression was observed, down from the 24.5-fold increase after LPS treatment to a 6.5-fold increase (Fig. 7A), or in the case of *Ccr1*, where a 198% decrease in gene expression was detected (Fig. 7B). Interestingly, rosuvastatin alone did not exhibit a strong effect on these latter genes, but only when activated by LPS (Fig. 7C, D). Other genes were regulated synergistically by rosuvastatin when applied to LPS-challenged microglia. For example, *Cxcl1* and *Ccl4* were both further upregulated by rosuvastatin in LPS-challenged cells (Fig. 7D, E). Some of the genes related to inflammation were not affected by the LPS challenge, but reacted weakly to rosuvastatin, as seen in *Hspb1* gene expression (Fig. 7G, H), where a 2.8-fold increase was detected.

DISCUSSION

We carried out a quantitative investigation of the complex morphological, functional and gene expression characteristics of pure microglial cells of embryonic origin after rosuvastatin treatment in unstimulated and LPS-challenged cultures, and highlighted the complex beneficial effects of rosuvastatin that make it an excellent candidate for preventive neuroinflammatory therapy with well-balanced properties of enhanced anti-inflammatory and subdued pro-inflammatory effects.

Although microglial cells prepared from embryonic nervous tissue may differ from those of the adult brain in certain characteristics (Floden and Combs, 2006), they are nevertheless similarly responsive to immunological (LPS) challenge and suitable for morphological, functional and gene expression studies. When activated, the microglia display both pro- and anti-inflammatory properties as they can be polarized along a continuum toward a detrimental (M1) or a beneficial (M2) state in the injured CNS (Kroner et al., 2014). Inflammation that is mediated, and perhaps enhanced, by the microglia has been implicated in a number of neuropathological conditions, ranging from acute injuries (Loane and Byrnes, 2010) and chronic inflammatory conditions (Gay, 2007; Napoli and Neumann, 2010) to neurodegenerative diseases (Long-Smith et al., 2009; Prokop et al., 2013).

Statins are commonly used in the treatment of high blood cholesterol levels (Burg and Espenshade, 2011). They are classified on the basis of their lipid-lowering efficacy and their lipophilic/hydrophilic nature (Hamelin and Turgeon, 1998; Jones et al., 1998; Davidson, 2002; Schachter, 2005); while lipophilic statins penetrate the cell membrane, hydrophilic statins such as rosuvastatin (Crestor; AstraZeneca Pharmaceuticals, LP, Wilmington, DE, USA) are transported through the blood–brain barrier via multiple transporters (Kitamura et al., 2008; Abbott et al., 2010; Ellis et al., 2013) or ATP-binding cassette efflux transporters in microglia (Gibson et al., 2012). Rosuvastatin exhibits the greatest inhibitory effect on cholesterol biosynthesis (McTaggart et al., 2001) and most favorably alters the high-density lipoprotein profile among statins (Asztalos et al., 2007); it was the fourth highest-selling prescription drug in the USA in 2013 (http://www.drugs.com/stats/top100/2013/sales).

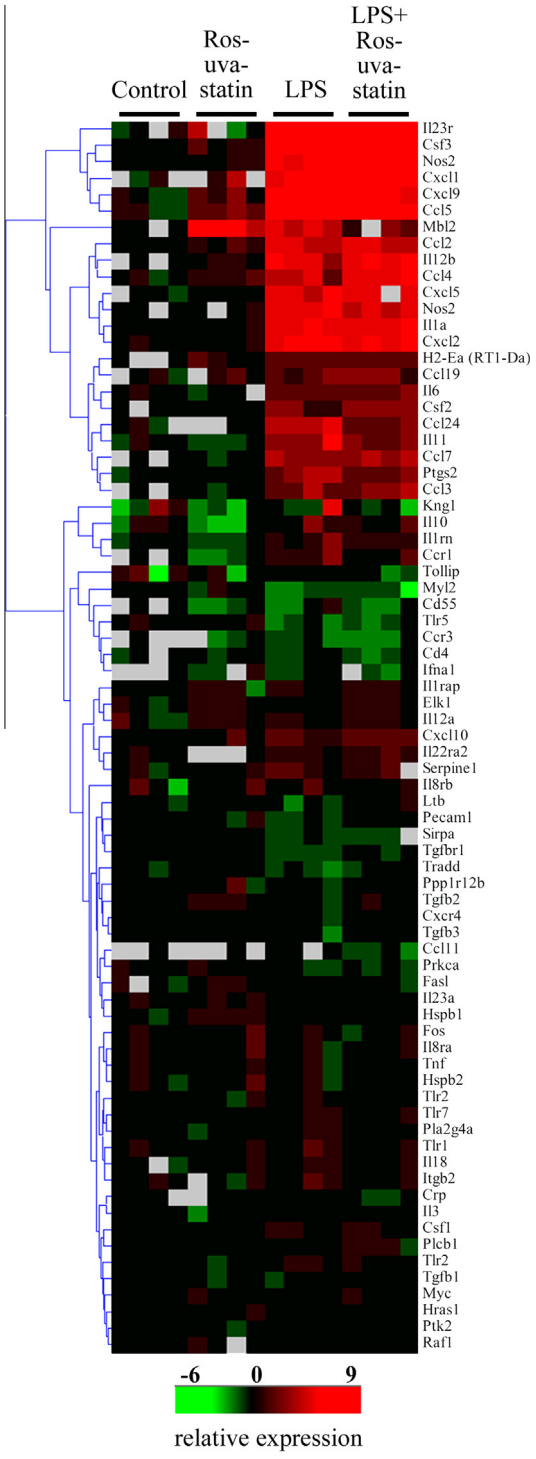

Fig. 6. Hierarchical cluster analysis of inflammation-related genes. Pure microglial cultures (subDIV4) were maintained and treated as described in Experimental procedures section. The cells (subDIV4) were cultured with or without LPS for 24 h in the presence or absence of rosuvastatin. Rosuvastatin: 1 μM; LPS: 20 ng/ml; LPS + rosuvastatin: LPS (20 ng/ml) + rosuvastatin (1 μM). For hierarchical cluster analysis and visualization, the Hierarchical Clustering Explorer (v3.0) software was used. The complete linkage clustering method was applied with Euclidean distance metric. The heat map depicts expression values relative to control samples on a $\log_2$ scale (overexpression: red, repression: green and no change: black). Missing values are indicated in gray. (For interpretation of the references to colour in this figure legend, the reader is referred to the web version of this article.)

Although their main action is to block cholesterol synthesis, other effects of statins, including those on the regression of atherosclerotic coronary lesions, are also important (Wierzbicki et al., 2003). Expecting similarly beneficial effects on the microglia, we determined how rosuvastatin modulates both pro- and anti-inflammatory actions by affecting numerous morphological, functional and gene expression parameters in pure microglial cultures. These cultures provide a unique opportunity to study these functional and expression parameters without the significant influence of any contaminating cell types. Our secondary microglial cultures were >99% pure, a crucial factor when levels of secreted pro- and anti-inflammatory peptides or gene expression levels are measured, as other cell types in the CNS are also capable of expressing such peptides (Gruol et al., 2014).

Our studies revealed the effects of rosuvastatin on various quantitative morphological properties of the microglia. Rosuvastatin affected the area, perimeter and TI profoundly in both unchallenged and LPS-challenged cells. It generally promoted microspike formation and increased the cell perimeter and TI through ramification. Concomitantly with the increase in cell area in both unchallenged and LPS-challenged cells, rosuvastatin affected the protein synthesis of Iba1, a protein that is implicated in actin cytoskeleton remodeling (Sasaki et al., 2001; Ohsawa et al., 2004). As expected, LPS treatment caused microglia activation that resulted in a low TI, but the combined treatment with LPS + rosuvastatin inhibited this activation through the development of microspikes and the cells becoming more ramified.

Rosuvastatin strongly inhibited microglia proliferation and adhesion as it significantly decreased the number of cells in both naïve and LPS-challenged cultures. Although the precise mechanisms are not known, statins are able to inhibit mitosis through cell cycle arrest in G1 (Yang et al., 2008) and G2/M (Gao et al., 2012). As rosuvastatin displays a weak anti-mitogenic effect, its regular use may prove helpful in lowering the risks of a number of cancer types (Simon et al., 2012). To quantify cell adhesion, we used the cell index value (Atienza et al., 2005; Jarvis et al., 2011). Our finding that rosuvastatin lowered cell adhesion in both unchallenged and LPS-challenged cells is in harmony with previous reports on the ability of statins to decrease the expression of cell adhesion molecules (Weber et al., 1997; Wierzbicki et al., 2003).

We also examined how rosuvastatin altered fluid-phase phagocytosis. Phagocytosis is crucial in both the normal and the pathologic CNS as it efficiently eliminates foreign materials, apoptotic cells and cell debris (Kettenmann et al., 2011), and alteration of this clearance function could be harmful (Hickman and El Khoury, 2014; Lue et al., 2015). For example, pro-inflammatory phenotypes are linked to the phagocytic activity, and the blocking of phagocytosis may prevent some forms of inflammatory neurodegeneration, and might therefore be beneficial during infection, trauma, ischemia, neurodegeneration and aging (Neher et al., 2011; He et al., 2014). LPS is a strong activator of microglial phagocytosis (Nakamura, 2002; Lund et al., 2006; Szabo and Gulya, 2013). In our study, rosuvastatin

Table 1. Differentially expressed transcripts in rosuvastatin-treated pure microglial cells with or without LPS challenge

Gene	Name, NCBI reference sequence ID, RGD ID	Rosuvastatin	LPS	LPS + Rosuvastatin
Cxcl1	Chemokine ligand 1 (melanoma growth-stimulating activity, alpha) NM_030845.1, RGD ID 619869	+7.05	+111.55	+394.01
Csf3	Colony-stimulating factor 3 NM_017104.1 (old), NM_017104.2, RGD ID 2426	+2.9	+310.7	+321.7
Il23r	Interleukin 23 receptor XM_001072576.2, RGD ID 1586368	+2.12	+246.56	+268.81
Ccl5	Chemokine ligand 5 NM_031116.3, RGD ID 69069	+6.56	+146.97	+241.56
Nos2	Nitric oxide synthase U26686.1, RGD ID 3185	+1.82	+169.95	+135.48
Cxcl9	Chemokine ligand 9 NM_145672.4, RGD ID 628798	+3.82	+118.20	+100.95
Il12b	Interleukin 12B NM_022611.1, RGD ID 628704	+1.7	+42.0	+87.7
Cxcl2	Chemokine ligand 2 NM_053647.1, RGD ID 70069	+1.2	+75.4	+67.3
Il1a	Interleukin 1 alpha NM_017019.1, RGD ID 2890	+1.1	+45.3	+57.0
Ccl4	Chemokine ligand 4 NM_053858.1, RGD ID 620441	+3.33	+17.65	+51.0
Cxcl5	Chemokine ligand 5 (also known as Cxcl6) NM_022214.1, RGD ID 708540	+1.1	+54.9	+43.4
Ccl2	Chemokine ligand 2 NM_031530.1, RGD ID 3645	+2.34	+34.49	+33.27
Ccl7	Chemokine ligand 7 NM_001007612.1, RGD ID 1359152	−1.4	+12.4	+14.4
Ccl3	Chemokine ligand 3 NM_013025.2, RGD ID 3647	−1.3	+9.1	+11.4
Il6	Interleukin 6 M26744.1, RGD ID 2901	−1.1	+5.6	+8.4
Il11	Interleukin 11 NM_133519.4, RGD ID 621475	−1.99	+19.28	+7.40
Ptgs2	Prostaglandin endoperoxide synthase 2 NM_017232.3, RGD ID 620349	−1.2	+11.8	+7.2
Ccl19	Chemokine ligand 19 NM_001108661.1, RGD ID 1310336	+2.39	+5.21	+6.87
Mbl2	Mannose-binding lectin 2 NM_022704.2, RGD ID 67380	+126.17	+33.22	+6.46
Ccl24	Chemokine ligand 24 NM_001013045.1, RGD ID 1310245	+1.65	+24.55	+6.51
Cxcl10	Chemokine ligand 10 NM_139089.1, RGD ID 620209	+1.8	+4.5	+5.5
Il22ra2	Interleukin 22 receptor, alpha 2 NM_001003404.1, RGD ID 1303169	+1.1	+2.5	+4.0
Il10	Interleukin 10 NM_012854.2, RGD ID 2886	−3.97	+3.08	+2.69
Il1rn	Interleukin 1 receptor antagonist NM_022194.2, RGD ID 621159	−2.19	+3.76	+2.63
Tlr2	Toll-like receptor 2 NM_198769.2, RGD ID 735138	−1.5	+1.8	+2.1
Ccr1	Chemokine receptor 1 NM_020542.2, RGD ID 708446	−2.89	+3.88	+1.96
Traf2	Tnf receptor-associated factor 2 NM_001107815.2, RGD ID 1310457	+1.6	+1.9	+1.6
Mknk1	MAP kinase-interacting serine/threonine kinase 1 NM_001044267.1, RGD ID 1559603	+1.4	+1.6	+1.5
CD47	Cluster of differentiation 47 NM_019195.2, RGD ID 2308	−1.1	+1.3	+1.4
Pla2g4a	Phospholipase A2, group IVA (cytosolic, Ca-dependent) NM_133551.2, RGD ID 67366	−1.7	+1.7	+1.3
Tlr7	Toll-like receptor 7 EF032637.1, RGD ID 1563357	−1.2	+1.8	+1.3

(*continued on next page*)

Table 1 (*continued*)

Gene	Name, NCBI reference sequence ID, RGD ID	Rosuvastatin	LPS	LPS + Rosuvastatin
Ddit3	DNA-damage-inducible transcript 3 NM_001109986.1, RGD ID 62391	−1.3	+1.7	+1.3
Il18rap	Interleukin 18 receptor accessory protein XM_003750691.2, RGD ID 727867	+1.2	+1.7	+1.2
Hmgn1	High-mobility group nucleosome-binding domain 1 NM_001013184.1, RGD ID 1307761	+1.6	+1.2	+1.0
Scarb1	Scavenger receptor class B, member 1 NM_031541.1, RGD ID 2302	+1.1	−1.3	+1.0
Jun	Jun proto-oncogene NM_021835.3, RGD ID 2943	+1.2	−1.8	−1.1
Hspb1	Heat shock protein 1 NM_031970.3, RGD ID 61306	+2.79	−1.04	−1.19
Hc	Clathrin, heavy chain NM_019299.1, RGD ID 2364	+1.0	+1.1	−1.3
Tgfb3	Transforming growth factor, beta 3 NM_013174.2, RGD ID 3851	+1.2	−1.9	−1.4
Elmo1	Engulfment and cell motility 1 NM_001108415.1, RGD ID 1308182	−1.0	−1.7	−1.6
Prkca	Protein kinase C, alpha NM_001105713.1, RGD ID 3395	+1.3	−2.1	−1.7
Il10rb	Interleukin 10 receptor, beta NM_001107111.1, RGD ID 1560373	−1.4	−1.1	−1.9
Tgfbr1	Transforming growth factor, beta receptor 1 NM_012775.2, RGD ID 3852	−1.2	−2.5	−2.0
Sirpa	The signal-regulatory protein a NM_013016.2, RGD ID 3449	−1.5	−2.7	−2.8
Tlr5	Toll-like receptor 5 FJ750588.1, RGD ID 631351	−1.2	−3.0	−2.9
Ccl11	Chemokine ligand 11 NM_019205.1, RGD ID 3644	−1.2	−1.4	−3.0
Myl2	Myosin, light polypeptide 2 NM_001035252.1 (old), NM_001035252.2, RGD ID 1564245	−1.3	−4.4	−5.2

The National Center for Biotechnology Information (NCBI) Reference Sequence Database can be retrieved at http://www.ncbi.nlm.nih.gov/refseq/. A description of a gene function (RGD ID) can be found in The Rat Genome Database 2015 (Shimoyama et al., 2015) at http://rgd.mcw.edu/. Data are expressed as fold-change over the expression of unchallenged and untreated (control) microglial cells. Treatments had different effects on inflammation-related genes. LPS mostly induced the upregulation of genes as compared with the untreated control microglia. Rosuvastatin alone also had some effects on these genes. Combined treatment demonstrated that rosuvastatin had different effects on LPS-activated microglia cells: inhibited the effect of LPS on certain genes (e.g. *Ccl24*, *Ccr1*, *Kng1*, *Nos2*, *Il11*), while it had a synergistic effect with LPS on others (e.g. *Cxcl1*, *Ccl4*, *Il23r*).

inhibited phagocytosis completely in the LPS-challenged microglia, while it was ineffective in inhibiting the basal-level phagocytosis in unchallenged cells, indicating that rosuvastatin is a potent inhibitor of this function only in pro-inflammatory situations and does not alter the normal clearance of cell debris in a healthy tissue. Thus, rosuvastatin could be helpful when excess microglial activity could harm the nervous tissue.

Cytokines, important immunomodulators in the normal functioning of the CNS, can be released, among others, by the microglial cells. Cytokines can also be harmful: previous studies have shown that neurodegeneration originating through neuroinflammation is often elicited by activated microglia (McGeer and McGeer, 2003, 2010) through the release of different pro-inflammatory cytokines and chemokines (Hanisch, 2002). High levels of IL-1β could be observed, for instance, in the vicinity of amyloid plaques of AD patients (McGeer et al., 1993; Lindberg et al., 2005; Ghosh et al., 2013), where activated microglia accumulate (Rodriguez et al., 2014). Previous studies also suggested that statins reduce levels of some of the pro-inflammatory cytokines (Lindberg et al., 2005; Nakamichi et al., 2006; Veillard et al., 2006) and increase the anti-inflammatory cytokine IL-10 (Schönbeck and Libby, 2004). As expected, both pro- (IL-1β, TNF-α) and anti-inflammatory cytokines (IL-10) were increased in LPS-challenged cells as compared with the unchallenged (control) group. Rosuvastatin did not significantly affect the basal cytokine levels in unchallenged microglia, but strongly inhibited levels of the pro-inflammatory cytokines IL-1β and TNF-α when tested in LPS-challenged cells. Besides the inhibition of these pro-inflammatory agents, rosuvastatin exerted a direct anti-inflammatory effect by elevating the level of IL-10 in both unchallenged and LPS-challenged cells.

Effects of rosuvastatin on such diverse immune mechanisms of microglia as phagocytosis and cytokine production indicated a strong likelihood of its involvement in many other immune system-wide functions and possible effects on inflammation-related genes. We demonstrated that rosuvastatin, LPS and their combination had differential effects on the expression of inflammation-related genes. Several genes were upregulated after LPS challenge, confirming

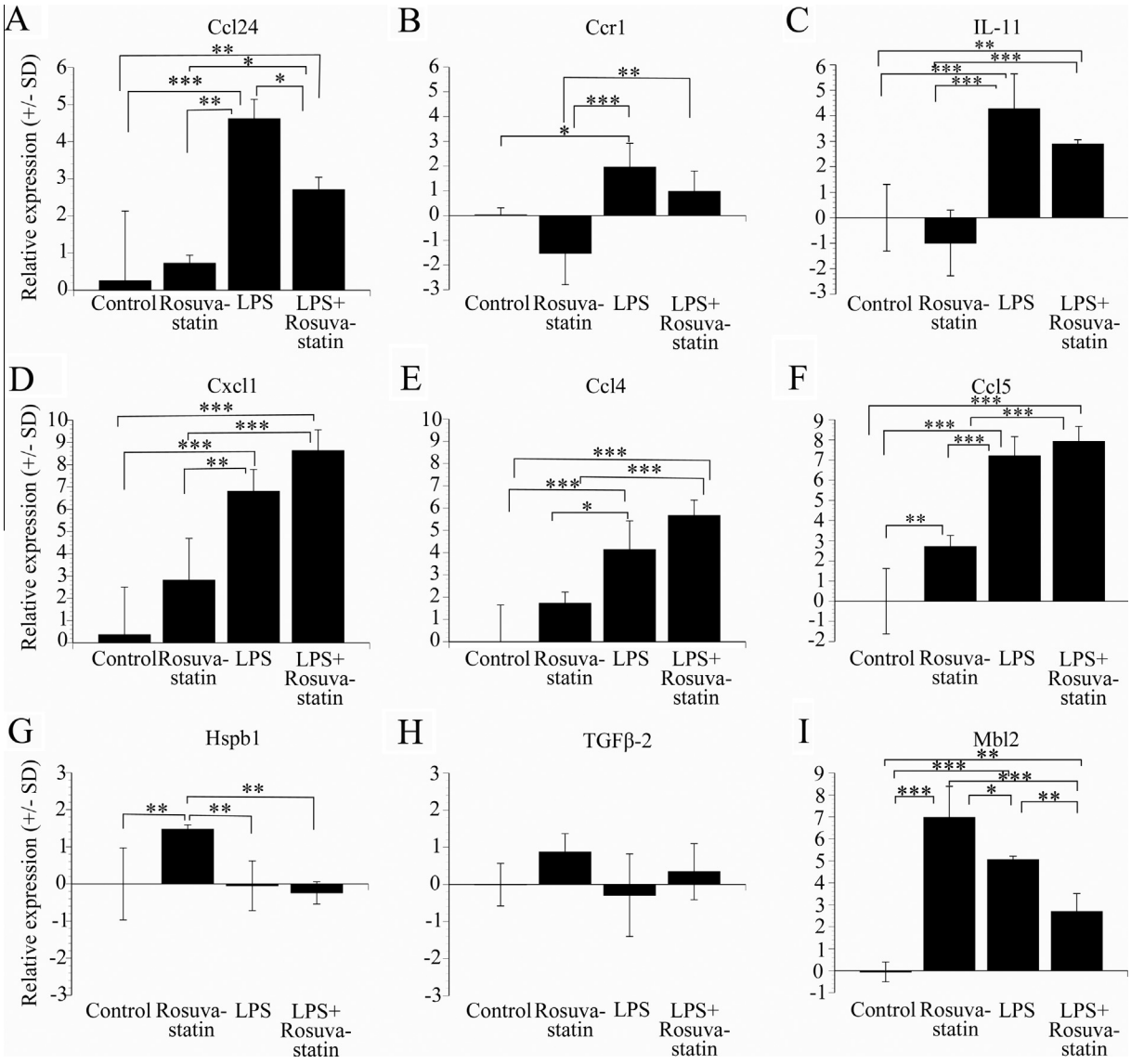

Fig. 7. Relative expression levels of various inflammation-related genes identified by real-time PCR in pure microglia cells. Pure microglial cultures (subDIV4) were maintained and treated as described in Experimental procedures section. The cells (subDIV4) were cultured with or without LPS for 24 h in the presence or absence of rosuvastatin. The extraction of total RNA and the real-time PCR are described in Experimental procedures section. The transcription levels of the chemokine ligand 24 (*Ccl24,* A), the chemokine receptor 1 (*Ccr1,* B), *IL-11* (C), the chemokine (CXC motif) ligand 1 (or melanoma growth-stimulating activity, alpha), (*Cxcl1*, D), the chemokine ligand 4 (*Ccl4*, E), the chemokine ligand 5 (*Ccl5*, F), the heat shock protein 1 (*Hspb1*, G), the transforming growth factor beta (*TGFβl-2*, H) and the mannose-binding lectin (protein C) 2 (*Mbl2*, I) are shown in unstimulated (control), LPS-challenged and LPS-challenged + rosuvastatin-treated cells. For some pro-inflammatory genes, rosuvastatin inhibited their expression which was upregulated in LPS-challenged cells. In connection with *Cxcl1*, *Ccl4* and *Ccl5*, the combined treatment revealed synergistic effects between rosuvastatin and LPS for Cxcl1, Ccl4 and Ccl5. Rosuvastatin increased levels of expression of *Hspb1*, *TGF-β* and *Mbl2*. Relative expression levels (on a $\log_2$ scale) ± SD from at least four separate experiments are shown for each condition. Data were analyzed with a two-way ANOVA. $^{*}p < 0.05$; $^{**}p < 0.01$; $^{***}p < 0.001$.

its strong pro-inflammatory effects on the microglia. Rosuvastatin itself and in combination with LPS displayed different effects on gene expression. Although rosuvastatin was not able to decrease all the LPS-upregulated genes, it suppressed the pro-inflammatory effects of LPS on some genes such as *Ccl24* or *Ccr1*. *Ccl24* is a chemokine that can readily be upregulated by pro-inflammatory cytokines or microbial stimulus such as LPS (Watanabe et al., 2002). *Ccr1* is implicated in multiple sclerosis (MS) and experimental autoimmune encephalomyelitis (EAE). Previous studies suggested that *Ccr1* could be upregulated in EAE (Rottman et al., 2000), and the microglia expressed Ccr1 around the demyelinating plaques, making Ccr1 antagonists or inhibitors possible targets for the development of MS-therapy (Hesselgesser et al., 1998; Eltayeb et al., 2007).

Rosuvastatin additionally increased the expression of certain genes. Its general effects on microglia were predominantly anti-inflammatory. The gene most upregulated by rosuvastatin was *Mbl2*, which is important in innate immunity (Worthley et al., 2005; Ip et al., 2009) and involved in the stimulation of phagocytosis (Stuart

et al., 2005). *Hspb1* was also upregulated by rosuvastatin. Hspb1 is a heat-shock protein with strong anti-apoptotic potential that regulates the cytoskeleton dynamics through F-actin stabilization (Concannon et al., 2003). Cxcl1 has been reported to be an anti-inflammatory protein with a neuroprotective role (Omari et al., 2009). Additional chemokine genes such as *Ccl2* (El Khoury et al., 2007; El Khoury and Luster, 2008), *Cxcl1* (Bosivert et al., 2006) and *Ccl5* were all upregulated in our studies and implicated in microglia recruitment to areas of inflammation. Although Ccl5 has been demonstrated to induce pro-inflammatory mechanisms (Skuljec et al., 2011), it has also been shown to ameliorate AD-like pathology by recruiting microglia to β-amyloid deposits (Lee et al., 2012). The expression of a number of phagocytosis-related gene was also tested. For example, *Mbl2* was upregulated in rosuvastatin-treated microglia in a seemingly contradictory action, while several other genes known to be involved in phagocytosis were inhibited, as expected from the phagocytosis essays, by rosuvastatin (for example *Myl2* (−1.27), *Sirpa* (−1.50), *Elmo1* (−1.05), or *CD47* (−1.07)). Although the overall downstream effect in the microglia is a strong inhibition of phagocytosis upon rosuvastatin treatment, it remains to be seen as to what intracellular signalization is activated to affect these genes or how these genes interact to elicit this particular cell response.

In summary, rosuvastatin elicits robust changes in the microglial functions *in vitro* as it potently inhibits the harmful pro-inflammatory signals and significantly enhances the beneficial anti-inflammatory actions of pure microglial cells after LPS challenge. Its effects include anti-mitogenic and anti-phagocytic action, strong inhibition of the synthesis of pro-inflammatory cytokines paralleled by a very strong stimulation of anti-inflammatory cytokine production, and a beneficial differential expression of a number of inflammation-related genes. As activated microglia often damage neuronal tissues by excessive cytokine and chemokine production and phagocytosis, the strong inhibition of such pro-inflammatory action by rosuvastatin illustrates an advantageous effect of this drug. Thus, rosuvastatin may be used prophylactically to inhibit pro-inflammatory and activate anti-inflammatory mechanisms of the microglia in order to reduce neuroinflammation and consequently neurodegeneration substantially. The microglia could therefore be a novel, specific therapeutic target in the fight against neurodegenerative disorders.

COMPETING INTERESTS

L.G.P. holds an equity position in Avidin Ltd. that produces a high-throughput QPCR product (Rat immune panel) and has a service using the same kit.

AUTHORS' CONTRIBUTIONS

This study is based on an original idea of K.G. L.H., L.G.P. and K.G. designed the experiments. D.K., I.F., L.Z.F. and L.H. performed research; L.G.P. contributed unpublished reagents/analytic tools; D.K., I.F. and L.H. analyzed data; D.K. and K.G. wrote the paper. All authors have read and approved the final manuscript.

Acknowledgments—This work was supported by program project grants to the University of Szeged from the Ministry of National Resources (TÁMOP-4.1.1.C-13/1/KONV-2014-0001, TÁMOP-4.2.1.B-09/1/KONV-2010-0005 and TÁMOP-4.2.2.A-11/1/KONV-2012-0052) through the European Union Cohesion Fund and from the National Development Agency of Hungary (KMR_12_1_2012_0072). The funders had no role in the study design, the data collection and analysis, the decision to publish, or the preparation of the manuscript. At the time of the experiments, D.K. was a Ph.D. student at the University of Szeged. We thank Mrs. Susan Ambrus for excellent technical help.

REFERENCES

Abbott NJ, Patabendige AA, Dolman DE, Yusof SR, Begley DJ (2010) Structure and function of the blood–brain barrier. Neurobiol Dis 37:13–25.

Ahmed Z, Shaw G, Sharma VP, Yang C, McGowan E, Dickson DW (2007) Actin-binding proteins coronin-1a and IBA-1 are effective microglial markers for immunohistochemistry. J Histochem Cytochem 55:687–700.

Asztalos BF, Le Maulf F, Dallal GE, Stein E, Jones PH, Horvath KV, McTaggart F, Schaefer EJ (2007) Comparison of the effects of high doses of rosuvastatin versus atorvastatin on the subpopulations of high-density lipoproteins. Am J Cardiol 99:681–685.

Atienza JM, Zhu J, Wang X, Xu X, Abassi Y (2005) Dynamic monitoring of cell adhesion and spreading on microelectronic sensor arrays. J Biomol Screen 10:795.

Banati RB, Gehrmann J, Schubert P, Kreutzberg GW (1993) Cytotoxicity of microglia. Glia 7:111–118.

Bodovitz S, Klein WL (1996) Cholesterol modulates alpha-secretase cleavage of amyloid precursor protein. J Biol Chem 271: 4436–4440.

Boisvert WA, Rose DM, Johnson KA, Fuentes ME, Lira SA, Curtiss LK, Terkeltaub RA (2006) Up-regulated expression of the CXCR2 ligand KC/GRO-alpha in atherosclerotic lesions plays a central role in macrophage accumulation and lesion progression. Am J Pathol 168:1385–1395.

Burg JS, Espenshade PJ (2011) Regulation of HMG-CoA reductase in mammals and yeast. Progr Lipid Res 50:403–410.

Concannon CG, Gorman AM, Samali A (2003) On the role of Hsp27 in regulating apoptosis. Apoptosis 8:61–70.

Cordle A, Landreth G (2005) 3-Hydroxy-3-methylglutaryl-coenzyme A reductase inhibitors attenuate β-amyloid-induced microglial inflammatory responses. J Neurosci 25:299–307.

Davidson MH (2002) Rosuvastatin: a highly efficacious statin for the treatment of dyslipidaemia. Exp Opin Invest Drugs 11:125–141.

El Khoury J, Luster AD (2008) Mechanisms of microglia accumulation in Alzheimer's disease: therapeutic implications. Trends Pharmacol Sci 29:626–632.

El Khoury J, Toft M, Hickman SE, Means TK, Terada K, Geula C, Luster AD (2007) Ccr2 deficiency impairs microglial accumulation and accelerates progression of Alzheimer-like disease. Nat Med 13:432–438.

Ellis LC, Hawksworth GM, Weaver RJ (2013) ATP-dependent transport of statins by human and rat MRP2/Mrp2. Toxicol Appl Pharmacol 269:187–194.

Eltayeb S, Berg AL, Lassmann H, Wallström E, Nilsson M, Olsson T, Ericsson-Dahlstrand A, Sunnemark D (2007) Temporal expression and cellular origin of CC chemokine receptors CCR1, CCR2 and CCR5 in the central nervous system: insight into mechanism of MOG-induced EAE. J Neuroinflamm 4:14.

Fabian G, Farago N, Feher LZ, Nagy LI, Kulin S, Kitajka K, Bito T, Tubak V, Katona RL, Tiszlavicz L, Puskas LG (2011) High-density

real-time PCR-based in vivo toxicogenomic screen to predict organ-specific toxicity. Int J Mol Sci 12:6116–6134.
Famer D, Wahlund LO, Crisby M (2010) Rosuvastatin reduces microglia in the brain of wild type and ApoE knockout mice on a high cholesterol diet; implications for prevention of stroke and AD. Biochem Biophys Res Commun 402:367–372.
Floden AM, Combs CK (2006) Beta-amyloid stimulates murine postnatal and adult microglia cultures in a unique manner. J Neurosci 26:4644–4648.
Fujita H, Tanaka J, Toin R, Tateishi N, Suzugl Y, Matsuda S, Sakanaka M, Maedap N (1996) Effects of GM-CSF and ordinary supplements on the ramification of microglia in culture: a morphometrical study. Glia 18:269–281.
Gamba P, Testa G, Gargiulo S, Staurenghi E, Poli G, Leonarduzzi G (2015) Oxidized cholesterol as the driving force behind the development of Alzheimer's disease. Front Aging Neurosci 7:119.
Gao Y, Lu XC, Yang HY, Liu XF, Cao J, Fan L (2012) The molecular mechanism of the anticancer effect of atorvastatin: DNA microarray and bioinformatic analyses. Int J Mol Med 30:765–774.
Gay F (2007) Activated microglia in primary MS lesions: defenders or aggressors? Int MS J MS Forum 14:78–83.
Gehrmann J, Matsumo Y, Kreutzberg G (1995) Microglia: intrinsic immunoeffector cell of the brain. Brain Res Rev 20:269–287.
Ghosh S, Wu MD, Shaftel SS, Kyrkanides S, LaFerla FM, Olschowka JA, O'Banion MK (2013) Sustained interleukin-1β overexpression exacerbates tau pathology despite reduced amyloid burden in an Alzheimer's mouse model. J Neurosci 33:5053–5064.
Gibson CJ, Hossain MM, Richardson JR, Aleksunes LM (2012) Inflammatory regulation of ATP binding cassette efflux transporter expression and function in microglia. J Pharmacol Exp Ther 343:650–660.
Ginhoux F, Greter M, Leboeuf M, Nandi S, See P, Gokhan S, Mehler MF, Conway SJ, Ng LG, Stanley ER, Samokhvalov IM, Merad M (2010) Fate mapping analysis reveals that adult microglia derive from primitive macrophages. Science 330:841–845.
Gonzalez-Scarano F, Baltuch G (1999) Microglia as mediators of inflammatory and degenerative diseases. Annu Rev Neurosci 22:219–240.
Graeber MB (2010) Changing face of microglia. Science 330: 783–788.
Gresa-Arribas N, Vieitez C, Dentesano G, Serratosa J, Saura J, Sola C (2012) Modelling neuroinflammation in vitro: a tool to test the potential neuroprotective effect of anti-inflammatory agents. Plos One 7:9.
Gruol DL, Vo K, Bray JG (2014) Increased astrocyte expression of IL-6 or CCL2 in transgenic mice alters levels of hippocampal and cerebellar proteins. Front Cell Neurosci 8:234.
Hamelin BA, Turgeon J (1998) Hydrophilicity/lipophilicity: relevance for the pharmacology and clinical effects of HMG-CoA reductase inhibitors. Trends Pharmacol Sci 19:26–37.
Hanisch UK (2002) Microglia as a source and target of cytokines. Glia 40:140–155.
He GL, Liu Y, Li M, Chen CH, Gao P, Yu ZP, Yang XS (2014) The amelioration of phagocytic ability in microglial cells by curcumin through the inhibition of EMF-induced pro-inflammatory responses. J Neuroinflamm 11:49.
Hesselgesser J, Ng HP, Liang M, Zheng W, May K, Bauman JG, Monahan S, Islam I, Wei GP, Ghannam A, Taub DD, Rosser M, Snider RM, Morrissey MM, Perez HD, Horuk R (1998) Identification and characterization of small molecule functional antagonists of the CCR1 chemokine receptor. J Biol Chem 273:15687–15692.
Hickman SE, El Khoury J (2014) TREM2 and the neuroimmunology of Alzheimer's disease. Biochem Pharmacol 88:495–498.
Ip WK, Takahashi K, Ezekowitz RA, Stuart LM (2009) Mannose-binding lectin and innate immunity. Immunol Rev 230:9–21.
Jarvis GE, Bihan Hamaia S, Pugh N, Ghevaert JG, Pearce C, Hughes CE, Watson SP, Ware J, Rudd E, Farndale RW (2011) A role for adhesion and degranulation-promoting adapter protein in collagen-induced platelet activation mediated via integrin $\alpha_2\beta_1$. J Thromb Haemost 10:268–277.
Jones P, Kafonek S, Laurora I, Hunninghake D (1998) Comparative dose efficacy study of atorvastatin versus simvastatin, pravastatin, lovastatin, and fluvastatin in patients with hypercholesterolemia (the CURVES study). Am J Cardiol 81: 582–587.
Kettenmann H, Hanischuk Noda M, Verkhratsky A (2011) Physiology of microglia. Physiol Rev 91:461–553.
Kitamura S, Maeda K, Wang Y, Sugiyama Y (2008) Involvement of multiple transporters in the hepatobiliary transport of rosuvastatin. Drug Metab Dispos 36:2014–2023.
Kreutzberg GW (1996) Microglia: a sensor for pathological events in the CNS. Trends Neurosci 19:312–318.
Kroner A, Greenhalgh AD, Zarruk JG, Passos Dos Santos R, Gaestel M, David S (2014) TNF and increased intracellular iron alter macrophage polarization to a detrimental M1 phenotype in the injured spinal cord. Neuron 83:1098–1116.
Kurata T, Miyazaki K, Kozuki M, Morimoto N, Ohta Y, Ikeda Y, Abe K (2012) Atorvastatin and pitavastatin reduce senile plaques and inflammatory responses in a mouse model of Alzheimer's disease. Neurol Res 34:601–610.
Lee JK, Schuchman EH, Jin HK, Bae JS (2012) Soluble CCL5 derived from bone marrow-derived mesenchymal stem cells and activated by amyloid β ameliorates Alzheimer's disease in mice by recruiting bone marrow-induced microglia immune responses. Stem cells 30:1544–1555.
Lindberg C, Crisby M, Winblad B, Schultzberg M (2005) Effects of statins on microglia. J Neurosci Res 82:10–19.
Loane DJ, Byrnes KR (2010) Role of microglia in neurotrauma. Neurother J Am Soc Exp Neurother 7:366–377.
Long-Smith CM, Sullivan AM, Nolan YM (2009) The influence of microglia on the pathogenesis of Parkinson's disease. Progr Neurobiol 89:277–287.
Lowry OH, Rosebrough NJ, Farr AL, Randall RJ (1951) Protein measurement with the folin phenol reagent. J Biol Chem 193: 265–275.
Lue LF, Schmitz C, Walker DG (2015) What happens to microglial TREM2 in Alzheimer's disease: immunoregulatory turned into immunopathogenic? Neuroscience 302:138–150.
Lund S, Christensen KV, Hedtjärn M, Mortensen AL, Hagberg H, Falsig J, Hasseldam H, Schrattenholz A, Pörzgen P, Leis M (2006) The dynamics of the LPS triggered inflammatory response of murine microglia under different culture and in vivo conditions. J Neuroimmunol 180:71–87.
Luo XG, Chen SD (2012) The changing phenotype of microglia from homeostasis to disease. Translat Neurodegener 1:9.
McGeer EG, McGeer PL (2003) Inflammatory processes in Alzheimer's disease. Progr Neuropsychopharm Biol Psychiatry 27:741–749.
McGeer EG, McGeer PL (2010) Neuroinflammation in Alzheimer's disease and mild cognitive impairment: a field in its infancy. J Alzheimers Dis 19:355–361.
McGeer PL, Kawamata T, Walker DG, Akiyama H, Tooyama I, McGeer EG (1993) Microglia in degenerative neurological disease. Glia 7:84–92.
McTaggart F, Buckett L, Davidson R, Holdgate G, McCormick A, Schneck D, Smith G, Warwick M (2001) Preclinical and clinical pharmacology of Rosuvastatin, a new 3-hydroxy-3-methylglutaryl coenzyme A reductase inhibitor. Am J Cardiol 87(5A):28B–32B.
Nakamichi K, Saiki M, Kitani H, Kuboyama Y, Morimoto K, Takayama-Ito M, Kurane I (2006) Suppressive effect of simvastatin on interferon-beta-induced expression of CC chemokine ligand 5 in microglia. Neurosci Lett 407:205–210.
Nakamura Y (2002) Regulating factors for microglial activation. Biol Pharm Bull 25:945–953.
Nakamura Y, Si QS, Kataoka K (1999) Lipopolysaccharide-induced microglial activation in culture: temporal profiles of morphological change and release of cytokines and nitric oxide. Neurosci Res 35:95–100.
Napoli I, Neumann H (2010) Protective effects of microglia in multiple sclerosis. Exp Neurol 225:24–28.

Neher JJ, Neniskyte U, Zhao JW, Bal-Price A, Tolkovsky AM, Brown GC (2011) Inhibition of microglial phagocytosis is sufficient to prevent inflammatory neuronal death. J Immunol 186:4973–4983.
Nicholls SJ, Ballantyne CM, Barter PJ, Chapman MJ, Erbel RM, Libby P, Raichlen JS, Uno K, Borgman M, Wolski K, Nissen SE (2011) Effect of two intensive statin regimens on progression of coronary disease. N Engl J Med 365:2078–2087.
Nissen SE, Nicholls SJ, Sipahi I, Libby P, Raichlen JS, Ballantyne CM, Davignon J, Erbel R, Fruchart JC, Tardif JC, Schoenhagen P, Crowe T, Cain V, Wolski K, Goormastic M, Tuzcu EM, ASTEROID Investigators (2006) Effect of very high-intensity statin therapy on regression of coronary atherosclerosis: the ASTEROID trial. JAMA 295:1556–1565.
Ohsawa K, Imai Y, Sasaki Y, Kohsaka S (2004) Microglia/macrophage-specific protein Iba1 binds to fimbrin and enhances its actin-bundling activity. J Neurochem 88:844–856.
Omari KM, Lutz SE, Santambrogio L, Lira SA, Raine CS (2009) Neuroprotection and remyelination after autoimmune demyelination in mice that inducibly overexpress CXCL1. Am J Pathol 174:164–176.
Ozsvári B, Puskás LG, Nagy LI, Kanizsai I, Gyuris M, Madácsi R, Fehér LZ, Gerö D, Szabó C (2010) A cell-microelectronic sensing technique for the screening of cytoprotective compounds. Int J Mol Med 25:525–530.
Prokop S, Miller KR, Heppner FL (2013) Microglia actions in Alzheimer's disease. Acta Neuropathol 126:461–477.
Rodriguez GA, Tai LM, LaDu MJ, Rebeck GW (2014) Human APOE4 increases microglia reactivity at Aβ plaques in a mouse model of Aβ deposition. J Neuroinflammation 11:111.
Rottman JB, Slavin AJ, Silva R, Weiner HL, Gerard CG, Hancock WW (2000) Leukocyte recruitment during onset of experimental allergic encephalomyelitis is CCR1 dependent. Eur J Immunol 30:2372–2377.
Sasaki Y, Ohsawa K, Kanazawa H, Kohsaka S, Imai Y (2001) Iba1 Is an actin-cross-linking protein in macrophages/microglia. Biochem Biophys Res Commun 286:292–297.
Schachter M (2005) Chemical, pharmacokinetic and pharmacodynamic properties of statins: an update. Fundam Clin Pharmacol 19:117–125.
Schönbeck U, Libby P (2004) Inflammation, immunity, and HMG-CoA reductase Inhibitors: statins as antiinflammatory agents. Circulation 109(S1):II18–II26.
Shimoyama M, De Pons J, Hayman GT, Laulederkind SJ, Liu W, Nigam R, Petri V, Smith JR, Tutaj M, Wang SJ, Worthey E, Dwinell M, Jacob H (2015) The Rat Genome Database 2015: genomic, phenotypic and environmental variations and disease. Nucleic Acids Res 43(Database issue):D743–D750.
Shobab LA, Hsuing GY, Feldman HH (2005) Cholesterol in Alzheimer's disease. Lancet Neurol 4:841–852.
Simon MS, Rosenberg CA, Rodabough RJ, Greenland P, Ockene I, Roy HK, Lane DS, Cauley JA, Khandekar J (2012) Prospective analysis of association between use of statins or other lipid-lowering agents and colorectal cancer risk. Ann Epidemiol 22:17–27.
Simons M, Keller P, De Strooper B, Beyreuther K, Dotti CG, Simons K (1998) Cholesterol depletion inhibits the generation in hippocampal neurons. Proc Natl Acad Sci USA 95:6460–6464.
Skuljec J, Sun H, Pul R, Bénardais K, Ragancokova D, Moharregh-Khiabani D, Kotsiari A, Trebst C, Stangel M (2011) CCL5 induces a pro-inflammatory profile in microglia in vitro. Cell Immunol 270:164–171.
Streit WJ (2002) Microglia as neuroprotective immunocompetent cells of the CNS. Glia 40:133–139.
Stuart LM, Takahashi K, Shi L, Savill J, Ezekowitz RA (2005) Mannose-binding lectin-deficient mice display defective apoptotic cell clearance but no autoimmune phenotype. J Immunol 174:3220–3226. Erratum in: J Immunol 175:3447.
Szabo M, Gulya K (2013) Development of the microglial phenotype in culture. Neuroscience 241:280–295.
Taylor F, Huffman MD, Macedo AF, Moore TH, Burke M, Davey Smith G, Ward K, Ebrahim S (2013) Statins for the primary prevention of cardiovascular disease. Cochrane Database Syst Rev 1:CD004816. 2013.
van der Most PJ, Dolga AM, Nijholt IM, Luiten PGM, Eisel UL (2009) Statins: mechanisms of neuroprotection. Progr Neurobiol 88:64–75.
Veillard NR, Braunersreuther V, Arnaud C, Burger F, Pelli G, Steffens S, Mach F (2006) Simvastatin modulates chemokine and chemokine receptor expression by geranylgeranyl isoprenoid pathway in human endothelial cells and macrophages. Atherosclerosis 188:51–58.
Watanabe K, Jose PJ, Rankin SM (2002) Eotaxin-2 generation is differentially regulated by lipopolysaccharide and IL-4 in monocytes and macrophages. J Immunol 168:1911–1918.
Weber C, Erl W, Weber KS, Weber PC (1997) HMG-CoA reductase inhibitors decrease CD11b expression and CD11b-dependent adhesion of monocytes to endothelium and reduce increased adhesiveness of monocytes isolated from patients with hypercholesterolemia. J Am Coll Cardiol 30:1212–1217.
Wierzbicki AS, Poston R, Ferro A (2003) The lipid and non-lipid effects of statins. Pharmacol Therap 99:95–112.
Worthley DL, Bardy PG, Mullighan CG (2005) Mannose-binding lectin: biology and clinical implications. Intern Med J 35: 548–555.
Woudstra C, Lambert D, Anniballi F, De Medici D, Austin J, Fach P (2013) Genetic diversity of the flagellin genes of Clostridium botulinum groups I and II. Appl Environ Microbiol 79:3926–3932.
Wu Y, Wu M, He G, Zhang X, Li W, Gao Y, Li Z, Wang Z, Zhang C (2012) Glyceraldehyde-3-phosphate dehydrogenase: a universal internal control for Western blots in prokaryotic and eukaryotic cells. Anal Biochem 423:15–22.
Yang YC, Huang WF, Chuan LM, Xiao DW, Zeng YL, Zhou DA, Xu GQ, Liu W, Huang B, Hu Q (2008) In vitro and in vivo study of cell growth inhibition of simvastatin on chronic myelogenous leukemia cells. Chemotherapy 54:438–446.
Zelcer N, Khanlou N, Clare R, Jiang Q, Reed-Geaghan EG, Landreth GE, Vinters HV, Tontonoz P (2007) Attenuation of neuroinflammation and Alzheimer's disease pathology by liver x receptors. Proc Natl Acad Sci USA 104:10601–10606.
Zipp F, Waiczies S, Aktas O, Neuhaus O, Hemmer B, Schraven B, Nitsch R, Hartung HP (2007) Impact of HMG-CoA reductase inhibition on brain pathology. Trends Pharmacol Sci 28:342–349.

(Accepted 23 November 2015)
(Available online 26 November 2015)